CGU HS Committee on River Ice Processes and the Environment
15th Workshop on River Ice
St. John's, Newfoundland and Labrador, June 15 - 17, 2009

Improved Satellite-Based River Ice Monitoring Using Dual-Polarized SAR Imagery

Karen Russell, Sherry Warren, Carl Howell, Thomas Puestow, Charles Randell
C-CORE Morrissey Road, St. John's, NL A1B 3X5
Karen.Russell@c-core.ca; Sherry.Warren@c-core.ca; Carl.Howell@c-core.ca
Thomas.Puestow@c-core.ca; Charles.Randell@c-core.ca
Ali Khan
NL Department of Environment and Conservation, St. John's, NL
Chandra Mahabir
Alberta Environment, Edmonton, Alberta
Patrick Tang
New Brunswick Department of Environment, Fredericton, NB
Dmitri Burakov
Hydrological Forecasts Department, Krasnoyarsk Region, Russia
Natalie Novik
Northern Forum, Anchorage, Alaska

C-CORE has been providing an operational Earth Observation (EO)-based river ice service using single polarized Synthetic Aperture Radar (SAR) imagery since 2003. Building on this experience, the capabilities of using dual-polarized ENVISAT Advanced Synthetic Aperture Radar (ASAR) imagery were investigated. Objectives of the current project included the evaluation of the utility of dual-polarized SAR data for river ice monitoring and the development of river ice classification algorithms for dual-polarized data for improved EO-based river ice monitoring. ENVISAT imagery collected from 2005-2008 were used during this study. Test sites included the Athabasca, Saint John, Exploits and Yenisei Rivers. Field data includes annotated maps, aerial and field photographs, aerial video, ice observer reports and emails from end users in the field. EO data and field data were correlated by date and location to identify suitable training sites. A quadratic discriminant classifier algorithm was developed based on image backscatter values and texture measures derived from the Grey Level Co-occurrence Matrix (GLCM). A sequential forward selection algorithm was employed to reduce the set of variables used in the classification. The results indicate the potential for improved ice class separability by incorporating both the HV channel and GLCM texture measures, confirming the utility of dual polarized SAR imagery for improved ice type discrimination.

1. Introduction

The development of ice covers on large rivers can result in ice jamming and extensive flooding. Decision makers require up-to-date information on river ice development to identify and mitigate potential hazards. Satellite based monitoring services offer an ideal method to collect information on river ice repeatedly and consistently throughout the ice season. Recently launched satellites, such as RADARSAT-2 provide a number of improved capabilities, such as higher spatial resolution, dual polarization mode, and full polarimetric data which could potentially enhance river ice monitoring services. A major motivation for this research was to improve the satellite-based river ice monitoring service currently delivered to a variety of end users under C-CORE's Polar View initiative, by evaluating the potential of dual-polarized SAR data for improved river ice classification.

2. Method

The available dual polarimetric data includes ground truthed ENVISAT scenes covering the entire ice season for the Athabasca River in Alberta, the Exploits River in Newfoundland, the Saint John River in New Brunswick, and the Yenisei River in Russia. Field data in the form of annotated maps, aerial and field photographs, aerial video, ice observer reports and emails were available for all study areas. The analysis consists of training site selection, SAR feature extraction, Sequential Forward Selection (SFS), quadratic discriminate performance, final classification and service implementation. A classification algorithm was developed using a pattern recognition approach for small sample size that follows from Raudys and Jain (1991) using a Quadratic Discriminant (QD). The results of the SFS and the QD functions were evaluated for both a region-based and a pixel-based approach. Confusion matrices were used to evaluate the overall classification accuracy.

2.1 Training Site Selection

River ice training sites were visually identified in the ENVISAT data based on geographic coordinates, both field and aerial photographs and descriptions provided by field personnel. Training site polygons were manually digitized using the HH and HV channels of 17 ENVISAT images. The training sites collected were organized into predefined ice classes that were identified in the SAR images and the validation data. The ice classes included open water, consolidated ice, intact ice and frazil ice. A total of 647 river ice samples were identified, with approximately 50 pixels each (See Table 1 and Figure 1). Due to limitations in the availability of validation data, the majority of these sites fall into the intact ice and water classes.

Previous river ice classification work under Polar View used a pixel-based classification approach, whereby each pixel in an image was evaluated and classified individually. However this approach does not take into account spatial variability or patterns within regions of an image. A region-based approach, which considers each training site as a single unit or region, can provide this additional information to improve classification accuracy. For this project, both a pixel-based and a region-based approach were evaluated.

2.2 SAR Feature Extraction

SAR image features or metrics that describe the ice classes were extracted for the training sites. These features are potentially useful for describing the classes by building statistical models that

represent an expected class signature. For the dual polarized data, the extracted features were based on the HH and HV polarization intensities, the intensity ratio, and the Grey Level Co-occurrence Matrix (GLCM) texture measures mean, entropy, homogeneity, and standard deviation, which were evaluated for both the HH and HV channels. Table 2 and Table 3 describe the features that were evaluated using the feature selection for the region and pixel based classifications.

2.3 Sequential Forward Selection

One of the fundamental problems in statistical pattern recognition is to determine which features should be employed for the best classification results (Raudys and Jain, 1991). Feature selection is a technique used to identify a subset of features, which perform best under a given classification system (Jain and Zongker, 1997). Feature selection algorithms cannot only reduce the cost of running a classification algorithm by reducing the feature space, but can also provide a better classification model due to the statically favored feature space that better fits the pattern recognition problem (Jain and Chandrasekaran, 1982).

The sequential forward selection (SFS) algorithm (Kittler, 1978; Aha and Bankert, 1996, Inza *et al.*, 2000) is a search method that starts with an empty feature set and iteratively evaluates and adds features in a forward manner. Once a feature has been identified as the best feature for the combination of feature space being evaluated, it is permanently assigned as a member of the selected set, and also removed from the possible features to be selected in the next phase of feature space search. This process continues until the inclusion of any of the remaining features does not yield an improvement to the classification.

For this analysis, SFS was applied three separate times to separate the river ice classes in the form of a binary decision tree. The binary tree format breaks an otherwise complex decision into a series of simpler decisions. The structure of the decision tree was built based on the HH intensity values. Figure 2 depicts the decision tree which was used to separate the river ice classes. At the first level of the tree all of the training data samples are classified as either ice or water. All of the samples which were labeled as ice are then passed onto the second level of the decision tree which further subdivides the ice types; this continues until all of the classes have been separated. This decision tree formed the basis for the structure of the classification algorithm.

2.4 Quadratic Discriminant (QD) Performance

It is important to estimate the classifier performance for evaluation and prediction purposes. The three main methods for performance estimation are re-substitution, hold out, and cross-validation (Raudys and Jain, 1991). For re-substitution, all samples are used to train the classifier and to test its performance. The hold out method separates all samples into two groups, a training set and a test set. The cross-validation method iteratively divides all samples into two groups, a training set and a test set. For each iteration of the cross-validation, a subset of data is extracted for training, and the remaining sample(s) are used for testing. The testing is such that each sample is tested only once during the entire process. The size of the testing subset can be as low as one sample.

2.5 Final Classification and Service Implementation

To implement the region based classification, a K-means segmentation algorithm was used to produce ice class regions. The K-means algorithm is one of the most commonly used segmentation methods due to its robustness and ease of implementation. This algorithm has some minor drawbacks, particularly the fact that it can be sensitive to the starting conditions (value of K and instance order) (Peña *et al*., 1999). However, the K-mean segmentation provides a starting point to initialize more intensive clustering or classification algorithms.

For the operational river ice classification, a K-means segmentation is applied to the HH intensity image and a 3 x 3 Kuan filter to reduce speckle (Kuan *et al*., 1987). The regions produced by the segmentation are passed into the classification algorithm, and are the basis for the region metrics used in the classification.

3. Results

Table 4 identifies variables that were selected using the SFS algorithm, and were subsequently selected for the classification of each ice class for both the pixel- (a) and region-based (b) approach. The primary contributing feature for each class discriminant is identified in the table, which makes the greatest contribution to the class discrimination. For both the pixel- and region-based approach the HH variables made the greatest contribution to separating the water and ice classes. However, the HV variables had a greater influence on the separation of the intact ice from the remaining ice classes. For the region-based approach, the key features used for the separation of the classes are HH intensity and HV intensity. The pixel-based approach relies primarily on the HH GLCM entropy and HV GLCM mean. Based on these initial results it is evident that the HV-related features are significant factors in discriminating between the river ice classes.

Figure 3 and Figure 4 compare the SFS accuracy rates of the potential classifier inputs, as evaluated by the cross-validation method. These graphs indicate that the HH+HV+GLCM combination produced the highest classifier accuracy rates for all river ice classes, for both the pixel- and region-based approaches. Using the HH channel alone particularly reduces the separability of the intact/light ice class from other ice classes. However, the HH+GLCM combination produced accuracy rates comparable to the HH+HV+GLCM combination for a region-based analysis. Overall, the region-based HH+HV+GLCM combination outperformed all other classifiers.

The accuracy rates for the region-based and pixel-based classification schemes using the HH, HV and GLCM combination were also evaluated by calculating confusion matrices. The region-based method, with an overall accuracy rate of 90.13%, outperformed the pixel-based method, which yielded an accuracy rate of 86.16% (See Table 5 and Table 6).

In both the region-based and pixel-based classification, water was the most accurately classified group. The three ice classes are more accurately classified by the region-based approach, particularly the intact/light ice class, which is classified correctly in 94.6% of the test cases, to 76% in the pixel-based approach. An example of the automated classification algorithm is shown in Figure 5. This algorithm produced good results, which corresponded well to the available

ground truth data. As shown in this figure, the separation of water-ice boundary appears accurate and well defined. Also, rough ice adjacent to the water is correctly classified.

4. Conclusion

The results of the dual polarization river ice classification algorithm show that the use of dual polarization SAR data provides improved river ice classification results over single polarization data. In particular, the introduction of the HV channel provides increased differentiation between ice types. Likewise, the use of texture measures provides an additional improvement to the dual polarization classification algorithm. Overall, a region-based approach using the combination of the HH and HV polarizations with the texture measures produced the highest accuracy rates.

Although the current dual-polarized classification algorithm shows promising results, additional adjustments to the algorithm should produce further improvements. The current results are based on a limited data set, with limited ground-truth for certain ice types. It is recommended that development of the dual-polarized classification algorithm continue, with additional SAR and ground-truth data from future river ice operations. Continued evaluation and fine-tuning of the image segmentation process is also recommended, in order to produce segments that correspond accurately with ice class features.

Acknowledgments

The authors would like to thank the Canadian Space Agency for providing funding support for this research and the European Space Agency for providing ENVISAT images. Thanks to the many end users of the Polar View River Ice Monitoring Service, who provided support and validation data: The NL Dept. of Environment and Conservation, New Brunswick Dept. of Environment, Alberta Environment, Faye Hicks, University of Alberta, the Krasnoyarsk Regional Government and the Northern Forum.

References

Aha, D. and Bankert, R., 1996. A comparative Evaluation of Sequential Feature Selection Algorithms. Learning from Data: AI and statistics. Edited by Fisher and Lenz.

Inza, I., Larranaga, P., Etxeberria, R., and Sierra, B. 2000. Feature Subset Selection by Bayesian network-based optimization, Artificial Intelligence vol.123, 157-184.

Jain, A. and Zongker, D. 1997. Feature Selection: Evaluation, Application, and Small Sample Performance, IEEE Transactions on pattern analysis and machine intelligence, vol. 19, no. 2.

Jain, A. and Chandrasekaran, B., 1982. Dimensionality and sample size considerations, In P. R. Krishnaiah and L. N. Kanal, editors, Pattern Recognition Practice, vol. 2, C.39, 835-855. North-Holland.

Kittler, J., 1978. Feature Set Search Algorithms, Pattern *Recognition and Signal Processing,* C.H. Chen, ed., 41-60. Sijthoff and Noordhoff, Alphen aan den Rijn, The Netherlands.

Kuan, D, Sawchuk, A, Strand, T. and Chavel, P. 1987. Adaptive restoration of images with speckle, IEEE Trans. ASSP., vol. 35, no. 3, 373-383.

Peña, J.M., Lozano, J.A., and Larrañaga, P., 1999. An empirical comparison of four initialization methods for the K-means algorithm. Pattern Recognition Letters. 20, 1027–1040.

Raudys, S.J. and Jain, A.K., 1991. Small sample size effects in statistical pattern recognition: recommendations for practitioners, Pattern Analysis and Machine Intelligence, IEEE Transactions, vol.13, no.3, 252-264.

Table 1 Number of training sites collected - by river and ice type.

		River				
		Athabasca	Exploits	Saint John	Yenisei	Total
Ice Type	Consolidated	16	66	8	0	90
	Intact	62	215	0	0	277
	Frazil	9	28	0	0	37
	Water	17	97	99	8	221
	Rapids	12	10	0	0	22
	Total	116	416	107	8	647

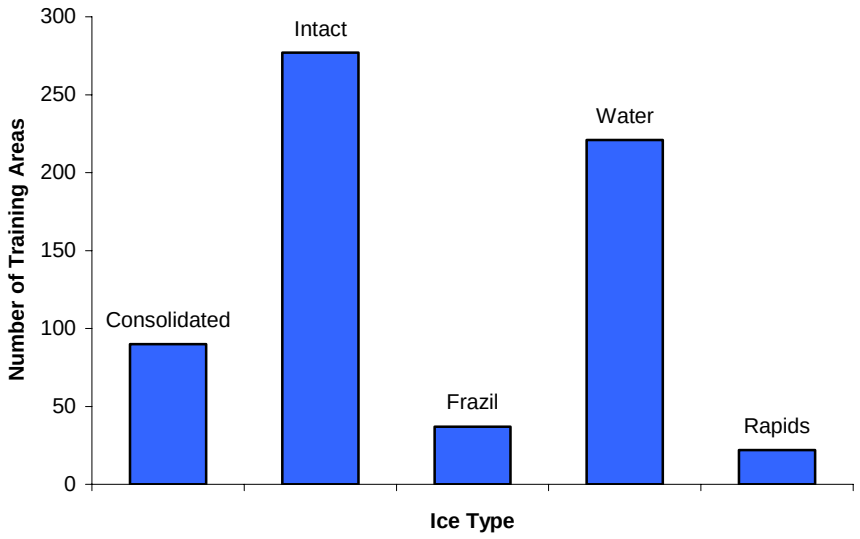

Figure 1 Frequency of ice classes in training data.

Table 2 SAR Features used in region-based classification development.

Feature	Description
HH (max)	HH Max intensity value for a region
HV (max)	HV Max intensity value for a region
HH (mean)	HH Mean intensity value for a region
HV (mean)	HV Mean intensity value for a region
HH (std)	HH Standard Deviation intensity value for a region
HV (std)	HV Standard Deviation intensity value for a region
HH/HV (mean)	Dual Cross-polarization ratio
HH/HV (max)	
HH/HV (std)	
HH GLCM Mean (mean)	Measure of local average grey level
HH GLCM Mean (max)	
HH GLCM Mean (std)	
HH GLCM Entropy (mean)	Measure of local entropy (disorder or randomness)
HH GLCM Entropy (max)	
HH GLCM Entropy (std)	
HH GLCM Homogeneity (mean)	Measure of local homogeneity (similarity of pixels)
HH GLCM Homogeneity (max)	
HH GLCM Homogeneity (std)	
HH GLCM Standard Deviation (mean)	Measure of grey level standard deviation
HH GLCM Standard Deviation (max)	
HH GLCM Standard Deviation (std)	
HV GLCM Mean (mean)	Measure of local average grey level
HV GLCM Mean (max)	
HV GLCM Mean (std)	
HV GLCM Entropy (mean)	Measure of local entropy (disorder or randomness)
HV GLCM Entropy (max)	
HV GLCM Entropy (std)	
HV GLCM Homogeneity (mean)	Measure of local homogeneity (similarity of pixels)
HV GLCM Homogeneity (max)	
HV GLCM Homogeneity (std)	
HV GLCM Standard Deviation (mean)	Measure of grey level standard deviation
HV GLCM Standard Deviation (max)	
HV GLCM Standard Deviation (std)	

Table 3 SAR Features used in pixel-based classification development.

Feature	Description
HH	HH intensity value
HV	HV intensity value
HH/HV	Dual Cross-polarization ratio
HH GLCM Mean	Measure of local average grey level
HH GLCM Entropy	Measure of local entropy (disorder or randomness)
HH GLCM Homogeneity	Measure of local homogeneity (similarity of pixels)
HH GLCM Standard Deviation	Measure of grey level standard deviation
HV GLCM Mean	Measure of local average grey level
HV GLCM Entropy	Measure of local entropy (disorder or randomness)
HV GLCM Homogeneity	Measure of local homogeneity (similarity of pixels)
HV GLCM Standard Deviation	Measure of grey level standard deviation

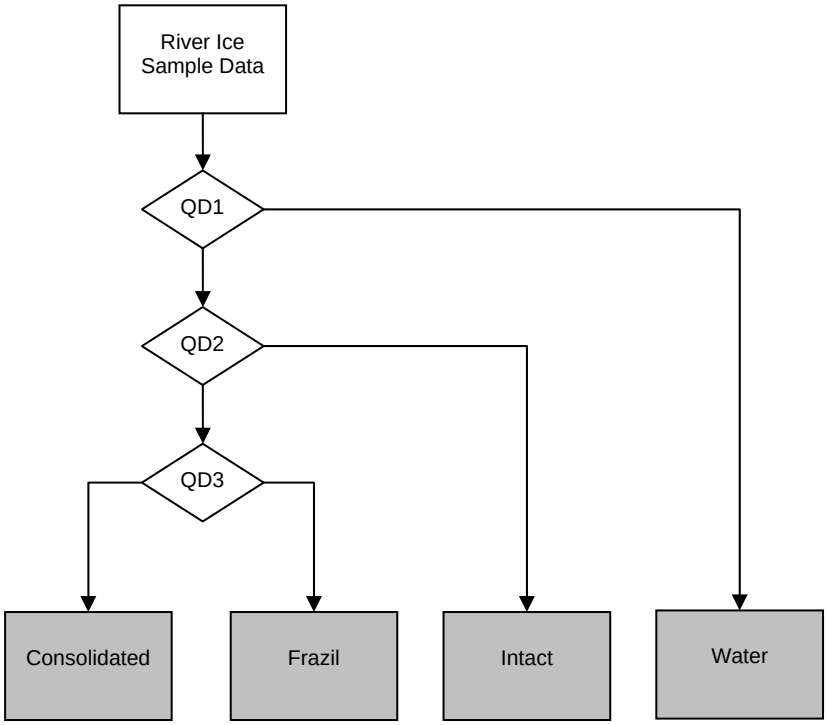

Figure 2 Classification structure based on a binary decision tree.

Table 4 Features identified using SFS for each level of the decision tree.

QD (Tree Level)	Primary feature	Other features
QD1	HH GLCM Entropy	HH GLCM Mean
QD2	HV GLCM Mean	HH(db), HV(db), HH GLCM Mean, HH GLCM Homogeneity
QD3	HV GLCM Mean	HH(db), HV(db), HH/HV Ratio, HH GLCM Mean, HV GLCM Mean, HV GLCM Entropy

(a) Pixel-based metrics identified by the SFS

QD (Tree Level)	Primary feature	Other features
QD1	HH(db)	HH GLCM Mean, HH GLCM Entropy
QD2	HV(db)	HH GLCM Mean, HH GLCM Entropy, HV GLCM Mean
QD3	HH(db)	HH/HV Ratio, HH GLCM Mean, HH GLCM Entropy, HV GLCM Entropy

(b) Region-based metrics identified by the SFS

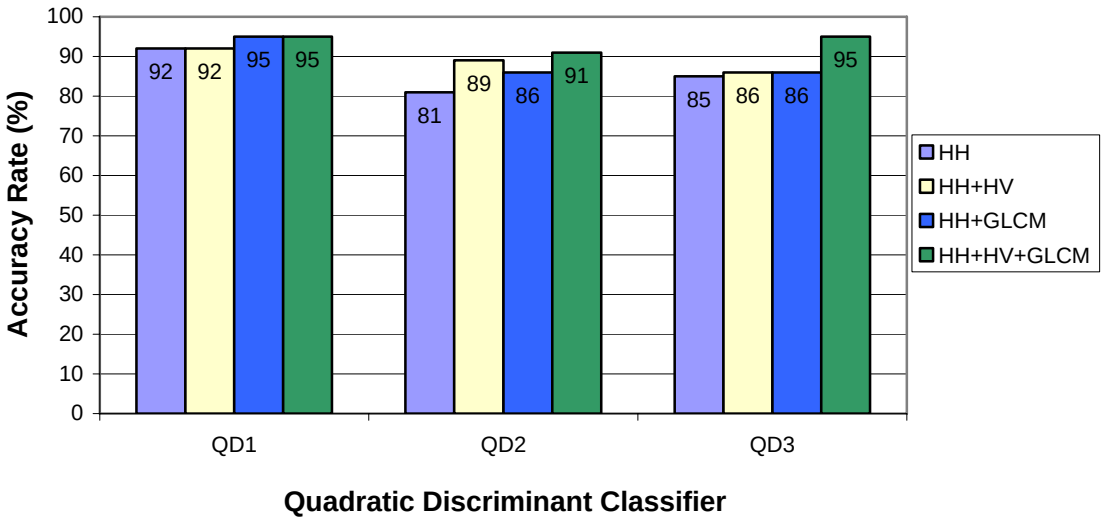

Figure 3 SFS accuracy rate comparison - region-based.

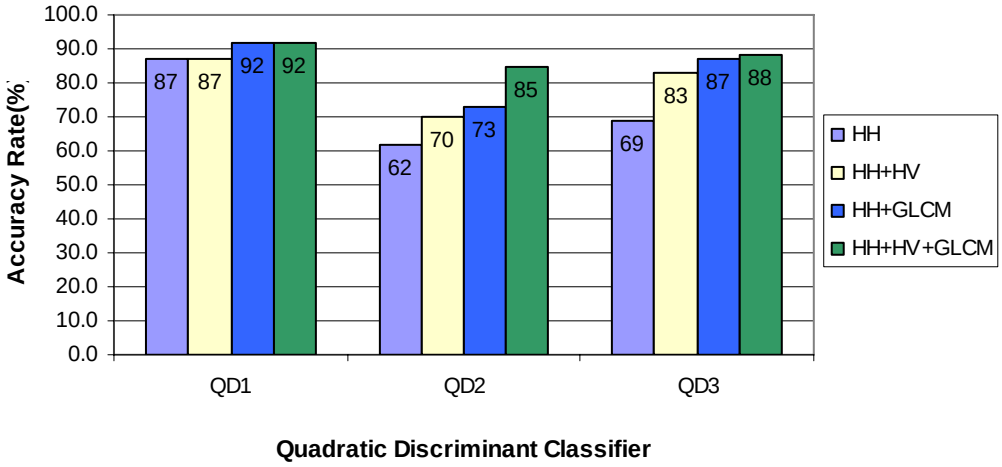

Figure 4 SFS accuracy rate comparison - pixel-based

Table 5 Confusion matrix of region-based classification results based on preliminary analysis.

		Actual				
		Water	Intact	Consolidated	Frazil	Total
Predicted	Water	192	1	0	0	193
	Intact	28	262	11	1	302
	Consolidated	0	13	70	3	86
	Frazil	1	1	1	24	27
	Total	221	277	82	28	608

Overall Accuracy = 90.13%

Table 6 Confusion matrix of pixel-based classification results based on preliminary analysis.

		Actual				
		Water	Intact	Consolidated	Frazil	Total
Predicted	Water	4828	70	107	69	5074
	Intact	238	1429	79	85	1831
	Consolidated	17	123	750	38	928
	Frazil	26	258	80	399	763
	Total	5109	1880	1016	591	8596

Overall Accuracy = 86.16%

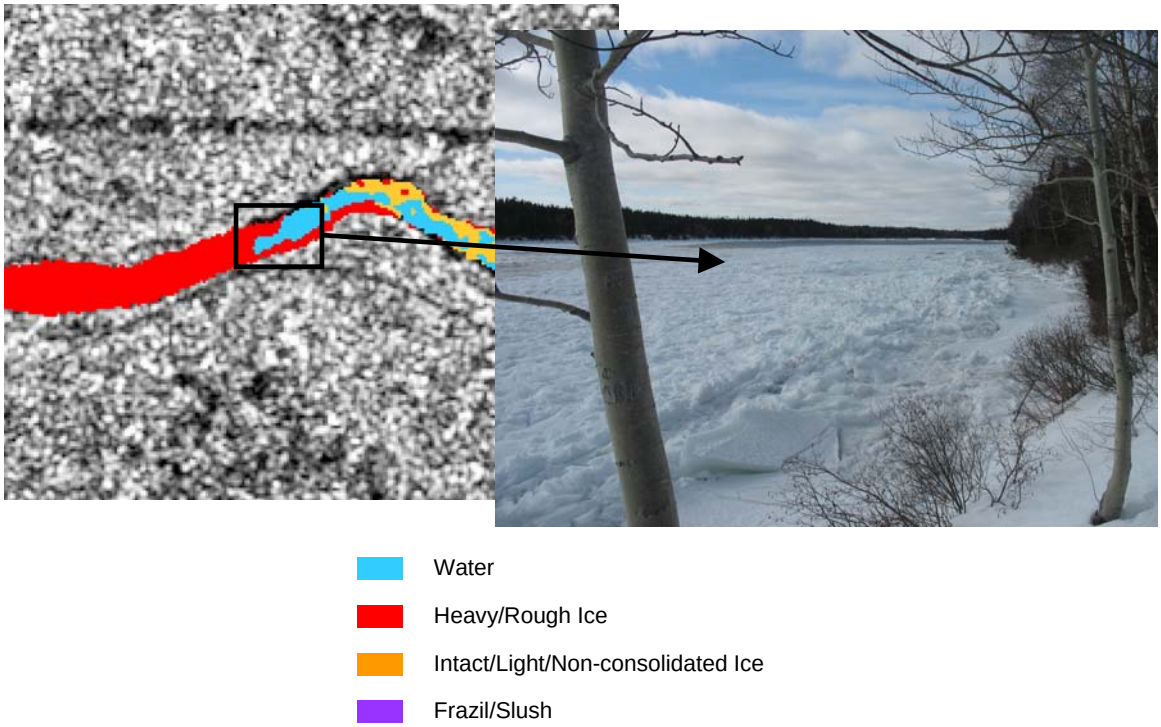

Figure 5 River ice classification of Exploits River segment displays good classification.